Thermochimica Acta 500 (2010) 44–50

Contents lists available at ScienceDirect

Thermochimica Acta

journal homepage: www.elsevier.com/locate/tca

# Effect of self-heating on photo-mechanical behavior of nematic elastomers

X. Jiang[a], T. Zhang[b], S. Ding[a], Y. Huo[a,*]

[a] Department of Mechanics and Engineering Science, Fudan University, 220 Handan Road, Shanghai, 200433, China
[b] Department of Mechanics, Peking University, Beijing, 100871, China

ARTICLE INFO

*Article history:*
Received 26 March 2009
Received in revised form 12 October 2009
Accepted 16 December 2009
Available online 24 December 2009

*Keywords:*
Nematic elastomer
Photo-isomerization
Nematic–isotropic transition
Photo-mechanical effect
Self-heating effect

ABSTRACT

The temperature increase due to self-heating and its effect on the photo-mechanical behavior were studied theoretically for photochromic nematic elastomers under light illumination. The sample temperature increase considered here is due to the heat released from the thermally activated back conversion of the azo dyes from the metastable, UV light-induced *cis* isomers to the stable *trans* isomers. A temperature equation is derived to include the self-heating effect. Our numerical calculations indicate that there exists a critical environment temperature, below which changes of the NI transition temperature caused by the photo-isomerization dominate the sample contractions and stresses. However, at higher environment temperatures, a sample temperature increase can produce larger contractions and stresses in mono-domain liquid crystal elastomers. The thermal effect is particularly strong near the initial nematic–isotropic transition temperature. Thus, the experimental reported photo-mechanical behavior is a coupled phenomenon of the thermal- and the photo-mechanical effects in general. More accurate thermal–mechanical experiments need be contacted to track this effect.

## 1. Introduction

Liquid crystal elastomers (LCE) are cross-linked polymeric materials with mesogenic liquid crystalline moieties. Nematic elastomer may exhibit rubber-like elastic behavior. The orientation change of its LC molecules at the nematic–isotropic (NI) transition temperature $T_{\mathrm{ni}}$ can induce a macroscopic shape change simultaneously by the interaction of the LC molecules with the backbone [1–5]. Thus, they can be used as active materials in various application fields such as artificial muscles, actuators and tunable optical devices [2–6]. For prolate LC polymers, the NI transition induces a macroscopic stretch along a director $\mathbf{n}$ and accompanied by a contraction on the perpendicular plane. Both the nematic order $Q$ and the stretch $\lambda$ along the director $\mathbf{n}$ are functions of the temperature difference $T_{\mathrm{ni}} - T$ in the nematic phase [7].

Photo-mechanical effects have been reported recently in photochromic nematic elastomers [8–12]. Large contractions up to 20% were obtained after irradiation by light with certain wavelength [8,9] for LCEs containing photoisomerizable groups, such as azobenzene. Recovery stress up to 2 kPa can be reached [10] for clamped samples. Photo-induced bending of LCE films is observed as well [11–13]. The effect is reversible through irradiations by lights with other wavelengths. This may lead to potential applications of a new type of light controllable artificial muscle system in sensors and microactuators.

The mechanism of such a photo-mechanical behavior has been primarily attributed to the effect of the photo-isomerization [8–10]. Azo dyes are rod-like and rigid in the equilibrium *trans* state, and thus contribute to the nematic order. They transform to the metastable *cis* state upon absorption of UV light, in which they are kinked. These kinked molecules will act as impurities and destabilize the liquid crystalline phase. As a result, the nematic–isotropic (NI) transition temperature $T_{\mathrm{ni}}$ is lowered, and the nematic order and the length of the sample are decreased [14,15].

Several associated effects exist during the above photo-isomerization process and they can have large influences on the photo-mechanical behavior. For example, the decay of the light intensity due to the absorption results in larger contractions near the surface, thus induces the bending of the photochromic nematic films [11–13,16–18]. For polarized light, the optical excitation depends strongly on the angle between the polarization vector of the light and the director of the LC phase [19,20]. This can induce anisotropic bending for poly-domain nematic films [11]. When the UV light is absorbed by the nematic elastomers with azo dyes, a part of the energy of the absorbed light heats the sample directly. The other part is utilized to transform the dye molecules from the lower energy *trans* to the higher energy *cis* configuration, thus to reduce the NI transition temperature $T_{\mathrm{ni}}$. Additional heat will be released when the molecules chemically convert back from *cis* to *trans*. The back conversion is inevitable because of the metastability of the

---

* Corresponding author. Tel.: +86 21 55664171; fax: +86 21 65642742.
*E-mail addresses:* yzhuo@fudan.edu.cn, yzhuo_cd@hotmail.com (Y. Huo).

0040-6031/$ – see front matter © 2009 Elsevier B.V. All rights reserved.
doi:10.1016/j.tca.2009.12.009

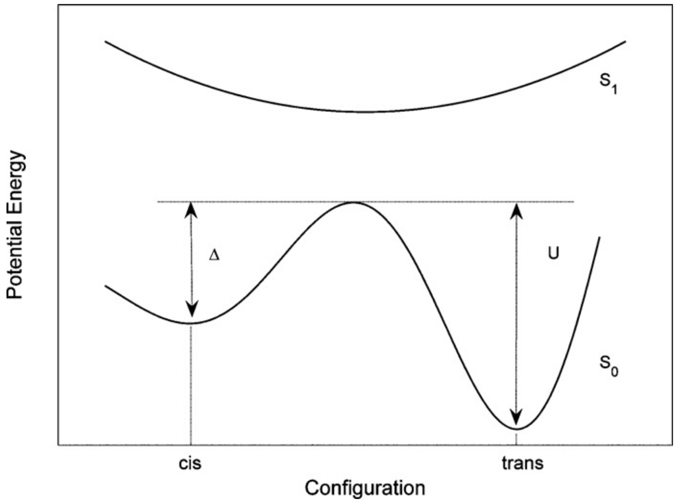

**Fig. 1.** Schematic potential energy landscape for the *trans-cis* transition of the azobenzene.

*cis* configuration. The self-heating and the direct heating raise the temperature of the sample as it is observed in experiments under isothermal conditions [9,10]. Accordingly, the nematic order $Q$ and the stretch $\lambda$ along the director $\mathbf{n}$ should be reduced. In poly-domain nematic elastomers, the effect of thermal-induced deformations of the differently oriented domains may cancel each other so as to conserve the overall shape. However, in mono-domain samples, this effect becomes significant macroscopically.

Although the temperature rise during the light irradiation was observed in experiments [9,10], the effect on the final deformation was not analyzed since it was not possible to separate the observed total deformation into thermal-induced and photo-induced parts. In this paper, we try to analyze the effect of the temperature change during the photo-mechanical process through phenomenological modeling and numerical calculations. After introducing the rate equation for the *trans-cis* isomerization and the formulae for calculating the light-induced shift of the NI transition temperatures, the energy changes during the process are considered and a temperature equation is derived. The thermal and the photo-mechanical induced deformations can be then calculated directly. It will be shown that in certain cases, the deformation due to self-heating can be rather large, even larger than the deformation due to the photochemical effect.

## 2. Model equations

### 2.1. Light-induced shift of NI transition temperatures

It is well known that the azobenzene chromophore can be reversibly switched by light at two wavelengths between an extended rod-like *trans* and a shorter kinked *cis* configuration. It is the basis for many experiments, in particular for various photo-mechanical behavior. Hugel et al. [21] reported recently that a single azobenzene polymer contracts under UV light and extends under visible light. Light-induced contractions in bulk polymers cross-linked with azobenzene was reported by Eisenbach [22] in 1980, but with rather small contractions (0.15–0.25%) comparing to the photochromic LCEs under considerations here.

The potential energy landscape of the azobenzene has been determined by ab initio calculations as well as from experiments [23,24]. As schematically shown in Fig. 1, the two configurations, *trans* in the right and *cis* in the left wells, are separated by an energy barrier in the ground state $S_0$ with $U$ much larger than $\varDelta$. The transition can be induced by optical excitations from $S_0$ to the first excited state $S_1$ with *trans* of 365 nm and *cis* of 420 nm wavelengths, respectively. Thus, the dynamics of the photo-isomerization process in LCEs containing azo dyes is governed by light-induced transition and the thermally induced transitions between the two configurations: *cis* and *trans*.

Let $n_0$ be the total number density of the azo dyes in the sample and $n_c$ the number density of the *cis* isomers, the number density of the *trans* configuration is $n_t = n_0 - n_c$. The following rate equation [8,9,19] can be used to calculate the population changes,

$$\frac{dn_c}{dt} = \frac{1}{\tau_t} n_t - \frac{1}{\tau_c} n_c + \eta_t I_t n_t - \eta_c I_c n_c. \tag{1}$$

The first two terms on the right hand side are the thermal excitation of *trans* to *cis* and the thermal relaxation from *cis* to *trans* with the temperature dependent characteristic times $\tau_t = \tau_0 \exp(U/kT)$ and $\tau_c = \tau_0 \exp(\varDelta/kT)$, respectively, where $U$ and $\varDelta$ are the corresponding energy barriers shown in Fig. 1. The last two terms are the transition rates due to the optical excitations with $\eta_t$ and $\eta_c$ the absorption coefficients for the light with the wavelength 365 nm and 420 nm, respectively. $I_t$ and $I_c$ are the corresponding light intensities. The absorption coefficients $\eta_t$ and $\eta_c$ may depend generally on the concentration of the photochromic molecules and the angles between the polarization direction of light and the rod axis of the trans isomers [8,19,20]. Here, for simplicity, we shall limit ourselves to consider only constant coefficients.

For isothermal light illumination process, the *cis* density can be solved analytically as

$$n_c(t) = n_c^{\infty} + (n_c(t=0) - n_c^{\infty}) \exp\left(\frac{-t}{\tau_{\text{eff}}}\right), \tag{2}$$

with the effective relaxation time and the saturated *cis* density depending on the temperature and the light intensities as

$$\frac{1}{\tau_{\text{eff}}} = \eta_t I_t + \eta_c I_c + \frac{1}{\tau_t} + \frac{1}{\tau_c} \quad \text{and} \quad n_c^{\infty} = n_0 \tau_{\text{eff}} \left(\frac{\eta_t I_t + 1}{\tau_t}\right). \tag{3}$$

Without light illuminations, the sample is in thermal equilibrium with the *cis* density as

$$n_c^0(T) = \frac{n_0}{(1 + \exp((U - \varDelta)/kT)))}. \tag{4}$$

The above equilibrium value is an increasing function of the temperature and should be very small, since the energy barrier $U$ is much bigger than $\varDelta$. From (2) and (3), when a sample is under the UV light illumination, i.e. $I_t > 0$ and $I_c = 0$, the *cis* population will increase exponentially due to the optical excitation from $n_c(t=0) = n_c^0(T)$ to the saturated value $n_c^{\infty}$. At the saturation, the UV light-induced *trans-cis* transition is balanced by the thermal-induced back conversion from *cis* to *trans*. If the UV light is switched off, the *cis* density will decrease exponentially back to the equilibrium value (4) due to the thermal-induced back conversion and the descending rate can be enhanced strongly by the visible light of 420 nm.

If the temperature varies during the light exposure, Eq. (1) must be solved numerically along with the temperature equation to be derived in the next subsection. However, once the kinked *cis* density $n_c$ is known, its effect on the NI transition temperature may be calculated from the following linear relation [8–10] as the first order approximation,

$$T_{\text{ni}}(n_c) = T_{\text{ni}}^0 - \beta n_c, \tag{5}$$

with $\beta$ a positive constant and $T_{\text{ni}}^0$ the initial NI transition temperature before light illuminations.

Although the NI transition in LC should be of the first order with discontinuous changes of the order parameter $Q$ and the shape of the samples at the transition temperature, the jumps have not been observed for cross-linked nematic elastomers [9,25,26]. The following empirical experimental fitting was proposed

$$Q = b(T_{\text{ni}} - T)^{\xi}, \tag{6}$$

for the nematic phase ($T \le T_{\text{ni}}$) with $\xi$ and $b$ two positive constants. For mono-domain LCEs, the stress-free uniaxial expansion $\lambda_{\text{m}} = L_{\text{m}}/L_{\text{i}}$ of the sample, with $L_{\text{m}}$ the present length and $L_{\text{i}}$ the length of the isotropic sphase can be well described by a linear relation, $\lambda_{\text{m}} = 1 + aQ$. Thus,

$$\lambda_{\text{m}} = 1 + \alpha(T_{\text{ni}} - T)^{\xi}, \tag{7}$$

with $\alpha = ab$ and $\xi$ two positive constants.

It is obvious from (6) and (7) that the decrease of $T_{\text{ni}}$ due to the light-induced *trans* to *cis* transition reduces $Q$ and $\lambda_{\text{m}}$. However, it is also clear that the raise of the temperature $T$ will have the same effect. It has been indeed observed in experiments that temperature always increases slightly (up to 9 °C) [9]. However, it was not possible to estimate how much of the observed sample deformations under light illuminations should be attributed to the temperature increase and how much is due to the shift of $T_{\text{ni}}$. To analyze these effects, the energy balance needs to be investigated.

### 2.2. Temperature equation

We start by considering the following energy balance equation for samples under light illuminations and placed in a heat reservoir with constant temperature (e.g. an oven),

$$\frac{de}{dt} = \dot{q} + \dot{w} + \dot{r}_{\text{light}}, \tag{8}$$

where $e$ is the internal energy density, $\dot{q}$ is the rate of the exchanging heat with the heat reservoir, $\dot{w}$ is the power of the external force and $\dot{r}_{\text{light}}$ is the power of the light radiations. The kinetic energy of the macroscopic motion is neglected.

For simplicity, we consider only samples with homogeneously distributed thermodynamic field variables: the temperature $T$, the nematic order $Q$ and the *cis* number density $n_{\text{c}}$. Moreover, only uniaxial loading will be considered with the Cauchy stress $\sigma$ and the extension $\lambda$. Space varying fields as in the light-induced bending experiments [11–13] may be taken into account by adding space derivatives in the temperature equation derived below. Thermal diffusion due to temperature gradients and its effect on the bending dynamics of nematic elastomers have been studied recently in [27].

We consider only ideal soft incompressible LCEs with entropy induced elasticity [1]. Namely, the elastical deformation will only change the entropy and the internal energy $e$ is independent of the extension $\lambda$ in the elastic range. According to (5) and (6), the nematic order is a function of the temperature and the *cis* density. Thus, we may assume that the internal energy density $e$ is a function of the temperature and the *cis* density, i.e. $e = e(T, n_{\text{c}})$. Its rate is

$$\frac{de}{dt} = c_{\text{p}}\frac{dT}{dt} + (U - \Delta)\frac{dn_{\text{c}}}{dt}, \tag{9}$$

where $c_{\text{p}}$ is the specific heat and $U - \Delta$ is the energy difference between the *cis* and the *trans* configurations as shown in Fig. 1.

Considering uniaxial loaded samples in a heat reservoir with the temperature $T_0$ and the heat exchanging coefficient $c$, the exchanging heat and the working power should be

$$\dot{q} = -c(T - T_0) \quad \text{and} \quad \dot{w} = \frac{\sigma}{\lambda}\frac{d\lambda}{dt}. \tag{10}$$

Note that the heat exchanging coefficient $c$ can depend on many factors such as the medium of the heat reservoir, the shape of the samples and the surfaces. In general, deformations can change the area and the shape of the surface. However, for simplicity, we shall not consider these effects and assume that the heat exchanging coefficient $c$ is a constant.

The absorbed radiation energy consists of two parts, the directly heating $\dot{r}_{\text{h}}$ of the sample and the energy needed for the *trans-cis* isomerization, $\dot{r}_{\text{tc}}$. $\dot{r}_{\text{h}}$ can be taken as proportional to the light intensity. From Fig. 1, the energy of formation of *trans-cis* transitions is $U - \Delta$ per molecule. By (1), the number fraction of the molecules in a sample that are isomerized by the light is $\eta_{\text{t}}I_{\text{t}}n_{\text{t}} - \eta_{\text{c}}I_{\text{c}}n_{\text{c}}$. Therefore,

$$\dot{r}_{\text{light}} = \dot{r}_{\text{tc}} + \dot{r}_{\text{h}},\ \dot{r}_{\text{tc}} = (U - \Delta)(\eta_{\text{t}}I_{\text{t}}n_{\text{t}} - \eta_{\text{c}}I_{\text{c}}n_{\text{c}}) \quad \text{and}$$
$$\dot{r}_{\text{h}} = \alpha_{\text{t}}I_{\text{t}} + \alpha_{\text{c}}I_{\text{c}}, \tag{11}$$

where $\alpha_{\text{t,c}}$ are positive constants. Now we insert (9)–(11) into (8), and use (1) to substitute $\dot{n}_{\text{c}}$ and yield the temperature equation for photochromic LCE samples under light illuminations as

$$c_{\text{p}}\frac{dT}{dt} = \frac{\sigma}{\lambda}\frac{d\lambda}{dt} - c(T - T_0) + \alpha_{\text{t}}I_{\text{t}} + \alpha_{\text{c}}I_{\text{c}} + (U - \Delta)\left(\frac{n_{\text{c}}}{\tau_{\text{c}}} - \frac{n_{\text{t}}}{\tau_{\text{t}}}\right). \tag{12}$$

Thus, the temperature change is governed by the power of the external force, the heat exchange with the environment, the direct and indirect heating of the light.

The photo-thermal–mechanical process of photochromic LCEs is governed by the photo-isomerization rate Eq. (1) for the *cis* population $n_{\text{c}}(t)$ and the energy balance Eq. (12) for the sample temperature $T(t)$. Then, the shift of the NI transition temperature can be calculated from (5) and the stress-free uniaxial extension can be completely evaluated from Eqs. (6) and (7) as

$$\lambda_{\text{m}}(t) = 1 + \alpha(T_{\text{ni}}^{0} - \beta n_{\text{c}}(t) - T(t))^{\xi}. \tag{13}$$

### 2.3. Heating effects

To analyze the indirect heating impact of radiation in detail, we may rewrite the photo-isomerization energy of light, $\dot{r}_{\text{tc}}$ given by (11.2) by the use of (1) as

$$\dot{r}_{\text{tc}} = (U - \Delta)\frac{dn_{\text{c}}}{dt} + (U - \Delta)\left(\frac{n_{\text{c}}}{\tau_{\text{c}}} - \frac{n_{\text{t}}}{\tau_{\text{t}}}\right).$$

The first term on the right hand side is essentially the internal energy change due to the *trans-cis* photo-isomerization, so cancels with the last term in (9) by considering the energy balance (8). The remaining term should be the indirect heating and can be reformulated by using $n_{\text{t}} = n_0 - n_{\text{c}}$ and (4) as

$$\dot{r}_{\text{tc}} = (U - \Delta)\frac{dn_{\text{c}}}{dt} + (U - \Delta)\left(\frac{1}{\tau_{\text{c}}} + \frac{1}{\tau_{\text{t}}}\right)(n_{\text{c}} - n_{\text{c}}^{0}(T)). \tag{14}$$

It is clear that in order to have a *cis* density $n_{\text{c}}$ larger than its thermal equilibrium value, $n_{\text{c}}^{0}(T)$, it is necessary to provide energies not only for the *cis-trans* transitions but also for keeping the difference of the *cis* density, $n_{\text{c}} - n_{\text{c}}^{0}$. The reason is that there is always a thermal activated back conversion from *cis* to *trans* until the population goes back to the thermal equilibrium value due to the metastability of the *cis* configuration. This back conversion produces heat, thus making for a self-heating effect.

Due to the direct- and the self-heating, the sample temperature always increases in the photo-mechanical processes. This can be clearly shown by considering the steady temperature of a sample under constant UV light exposure for an extensive time. Hence, all the time derivatives vanish in (12) and the steady temperature reads

$$T_{\infty} = T_0 + \frac{\alpha_{\text{t}}I_{\text{t}}}{c} + (U - \Delta)\left(\frac{1}{\tau_{\text{c}}} + \frac{1}{\tau_{\text{t}}}\right)\frac{(n_{\text{c}}^{\infty} - n_{\text{c}}^{0}(T_{\infty}))}{c}, \tag{15}$$

where $n_{\text{c}}^{\infty}$ is the saturated *cis* density given by Eq. (3.2). It is obvious that the final temperature has been increased through the direct heating (second term on the right) and self-heating (last term on the right) of the UV light illumination. A larger number density of the azo dyes and a higher light intensity will raise the temperature higher. A sample placed in an environment with lower heat exchanging coefficient $c$ such as in the air will experience larger temperature rise than in e.g. liquids.

In the following, the effect of the temperature increase due to the self-heating on the deformation and the stress of a sample will be studied in some details by numerical calculations to illustrate its importance. The direct heating effect is relatively straightforward and can be added easily.

## 3. Numerical results and discussions

### 3.1. Thermal and photo-induced contractions

Consider an unloaded photochromic LCE sample in an oven at a temperature $T_0$ and irradiated by UV light. The sample contracts because of the temperature increase $\delta T = T - T_0$ (the thermal–mechanical effect) and the NI transition temperature shift $\delta T_{\rm ni} = T_{\rm ni}^0 - T_{\rm ni}$ (the photo-mechanical effect). According to Eq. (7), the uniaxial expansion along the director $\mathbf{n}$ of the LCE sample in the nematic phase with respect to the isotropic phase is given by $\lambda_{\rm m} = L_{\rm m}/L_{\rm i} = 1 + \alpha(T_{\rm ni} - T)^{\xi}$. The contraction of the sample under light illuminations would be better characterized by the strain $\varepsilon_{\rm m} = (L_{\rm m} - L_{\rm m}^0)/L_{\rm m}^0$, with $L_{\rm m} = L_{\rm i}\lambda_{\rm m}$ the changed length and $L_{\rm m}^0 = L_{\rm i}\lambda_{\rm m}^0 = L_{\rm i}(1 + \alpha(T_{\rm ni}^0 - T_0)^{\xi})$ the initial length before the irradiation. By (7), the contraction is given by

$$\varepsilon_{\rm m} = \frac{\alpha(T_{\rm ni}^0 - T_0)^{\xi} - \alpha(T_{\rm ni} - T)^{\xi}}{1 + \alpha(T_{\rm ni}^0 - T_0)^{\xi}} = \frac{\alpha(T_{\rm ni}^0 - T_0)^{\xi}}{1 + \alpha(T_{\rm ni}^0 - T_0)^{\xi}}(1 - (1 - \delta\theta - \delta\theta_{\rm ni})^{\xi}), \tag{16}$$

where $\delta\theta = \delta T/(T_{\rm ni}^0 - T_0)$ and $\delta\theta_{\rm ni} = \delta T_{\rm ni}/(T_{\rm ni}^0 - T_0)$ are the normalized shifts. Since $\xi \sim 0.2$ for most LCEs [1,7,9], the contraction is highly nonlinear with respect to $\delta\theta$ and $\delta\theta_{\rm ni}$ except when they are very small. From their definition, one may define the thermal-induced and the photo-induced contractions as determined by $\delta\theta$ and $\delta\theta_{\rm ni}$, respectively. Namely,

$$\varepsilon_{\rm m}^{\rm th} = \frac{\alpha(T_{\rm ni}^0 - T_0)^{\xi}}{1 + \alpha(T_{\rm ni}^0 - T_0)^{\xi}}(1 - (1 - \delta\theta)^{\xi}) \quad \text{and}$$

$$\varepsilon_{\rm m}^{\rm ph} = \frac{\alpha(T_{\rm ni}^0 - T_0)^{\xi}}{1 + \alpha(T_{\rm ni}^0 - T_0)^{\xi}}(1 - (1 - \delta\theta_{\rm ni})^{\xi}). \tag{17}$$

#### 3.1.1. Steady state after long time irradiation

The steady value of the sample temperature under an extensive long time of the UV light illumination is given by (15). By using (2)–(4), the temperature increase due to the self-heating is

$$T_\infty = T_0 + \frac{U - \Delta}{c\tau_0}\exp\left(-\frac{\Delta}{kT_\infty}\right)\left(1 + \exp - \left(\frac{U - \Delta}{kT_\infty}\right)\right)(n_{\rm c}^\infty - n_{\rm c}^0),$$

$$\frac{(n_{\rm c}^\infty - n_{\rm c}^0)}{n_0} = \frac{\eta_{\rm t}I_{\rm t} + \tau_0^{-1}\exp(-(U/kT_\infty))}{\eta_{\rm t}I_{\rm t} + \tau_0^{-1}\exp(-(U/kT_\infty)) + \tau_0^{-1}\exp(-(\Delta/kT_\infty))} - \frac{\exp(-((U - \Delta)/kT_\infty))}{1 + \exp(-((U - \Delta)/kT_\infty))}.$$

To simplify the expression further, we make use of the parameters reported in [9], see Table 1 and the fact that $U >> \Delta$. Thus, we have that

$$\exp\left(-\frac{(U - \Delta)}{kT}\right) << 1 \quad \text{and} \quad \eta = \eta_t I_t \sim \tau_\circ^{-1}\exp(-\Delta/kT)$$

$$>> \tau_\circ^{-1}\exp\left(-\frac{U}{kT}\right)$$

for $T$ not very far from the room temperature. Thus, we may neglect all small terms and obtain the steady temperature as

$$T_\infty = T_0 + \frac{n_0(U - \Delta)}{c}\frac{\eta_{\rm t}I_{\rm t}\tau_0^{-1}\exp(-\Delta/kT_\infty)}{\eta_{\rm t}I_{\rm t} + \tau_0^{-1}\exp(-\Delta/kT_\infty)}. \tag{18}$$

**Table 1**

Model parameters adopted from [9].[a].

| $\eta_{\rm t}I_{\rm t}(s^{-1})$ | $\alpha$ | $\xi$ | $\beta n_0(K)$ | $\Delta(J)$ | $c/c_{\rm p}(s^{-1})$ | $n_0(U - \Delta)/c_{\rm p}(K)$ |
|---|---|---|---|---|---|---|
| $2.2 \times 10^{-4}$ | 0.22 | 0.195 | 11.8 | $4 \times 10^{-20}$ | $1.65 \times 10^{-3}$ | 36.4 |

[a] The first 5 are listed in IV. C. of [9]. The last 2 were obtained in the following way. The light-induced contraction given by (13) with $n_{\rm c}(t)$ and $T(t)$ obtained by solving (1) and (12) numerically depends on the two remaining parameters $c/c_{\underline{\rm p}}$ and $n_0(U - \Delta)/c_{\rm p}$, and the direct heating. As pointed out in [9], the measured temperature raise should mainly be attributed to the self-heating only (III. B. in [9]). Thus, we may define $\tilde{T}_0 = T_0 + \alpha_{\rm t}I_{\rm t}/c$ as the equilibrated temperature and adjust the only remaining two parameters to fit the calculated $T(t)$ and $\lambda_{\rm m}(t)$ with the experimental results of Fig. 4 in [9].

For any given environmental temperature $T_0$ (it is also the initial temperature of the sample), the steady temperature $T_\infty$ of the sample under the light illumination can be obtained as $T_\infty = \hat{T}_\infty(T_0)$ from this nonlinear and implicit algebraic equation.

The shift of the NI transition temperature is determined by (5). Together with (3) for the saturated *cis* population, the shift after long time of irradiation is

$$T_{\rm ni}^\infty = T_{\rm ni}^0 - \beta n_{\rm c}^\infty(T_\infty) = T_{\rm ni}^0 - \frac{\beta n_0\eta_{\rm t}I_{\rm t}}{\eta_{\rm t}I_{\rm t} + \tau_0^{-1}\exp(-\Delta/kT_\infty)}. \tag{19}$$

As shown in Fig. 2(a), both $T_\infty$ and $T_{\rm ni}^\infty$ are increasing functions of $T_0$ and $T_\infty < T_{\rm ni}^\infty$ until $T_0^{\rm M}$. For $T_0 \geq T_0^{\rm M}$, the sample is in the isotropic phase after the irradiation for which (7) is no longer valid and $\lambda_{\rm m} \equiv 1$. $T_0^{\rm M}$ can be obtained by solving the above two coupled equations for $T_\infty = T_{\rm ni}^\infty$.

Our numerical calculations yield $T_0^{\rm M} \approx 60.6\,^\circ\mathrm{C}$. The temperature increase $\delta T_\infty = T_\infty - T_0$ and the NI transition temperature shift $\delta T_{\rm ni}^\infty = T_{\rm ni}^0 - T_{\rm ni}^\infty$ are shown in Fig. 2(b). At temperatures much lower than the initial NI transition temperature, the temperature increase is rather small and it increases quasi-linearly with $T_0$ and catches the descending NI transition temperature shift at a critical environmental temperature $T_0^{\rm c}$. When $T_0 > T_0^{\rm c}$, we expect that the thermal effect is more dominant than the photo effect. The critical temperature $T_0^{\rm c}$ may be obtained by $\delta T_\infty/\delta T_{\rm ni}^\infty = 1$ and from Eqs. (18) and (19) as

$$T_0^{\rm c} = \frac{\Delta/k}{\ln((U - \Delta)/\beta\tau_0 c)} - \frac{\beta n_0\eta_{\rm t}I_{\rm t}}{\eta_{\rm t}I_{\rm t} + \beta c/(U - \Delta)}. \tag{20}$$

The critical temperature is $T_0^{\rm c} \approx 46.8\,^\circ\mathrm{C}$, well below $T_{\rm ni}^0 = 67\,^\circ\mathrm{C}$. However, it increases with the heat exchanging coefficient $c$ and decreases with the light intensity $I_{\rm t}$. For example, if $c$ is doubled, it will increase to $T_0^{\rm c} = 75.4\,^\circ\mathrm{C} > T_{\rm ni}^0$. Thus, the thermal effect should be negligible for thermal baths with very large heat exchanging coefficients such as liquids. However, the light propagation in a liquid medium may complicate the photo-mechanical phenomenon.

Fig. 3 shows the total contraction $\varepsilon_{\rm m}^\infty$, the thermal and photo-induced contractions, $\varepsilon_\infty^{\rm th}$, $\varepsilon_\infty^{\rm ph}$ and their sum $\varepsilon_\infty^{\rm th} + \varepsilon_\infty^{\rm ph}$. The photo-induced contraction $\varepsilon_\infty^{\rm ph}$ is larger than the thermal-induced one $\varepsilon_\infty^{\rm th}$ when the sample is under UV light irradiation at environmental temperatures lower than $T_0^{\rm c}$. At higher temperatures, the thermal effect becomes much more dominant.

#### 3.1.2. Evolution process under UV light illuminations

The evolution process of photochromic LCEs is governed by the two coupled ordinary differential Eqs. (1) and (12) for the *cis* popu-

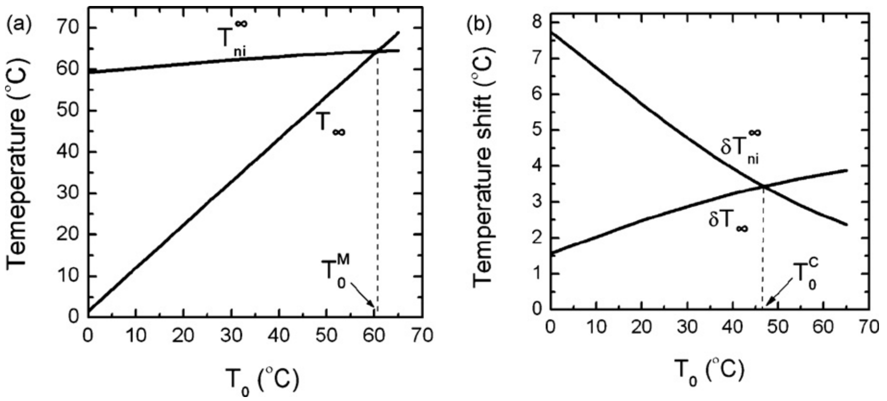

**Fig. 2.** Steady values of (a) the sample temperature $T_{\infty}$ and the NI transition temperature $T_{ni}^{\infty}$, (b) the shifts of the sample temperature $\delta T_{\infty} = T_{\infty} - T_0$ and the NI transition temperature $\delta T_{ni}^{\infty} = T_{ni}^{\circ} - T_{ni}^{\infty}$, as functions of the environmental temperature $T_0$.

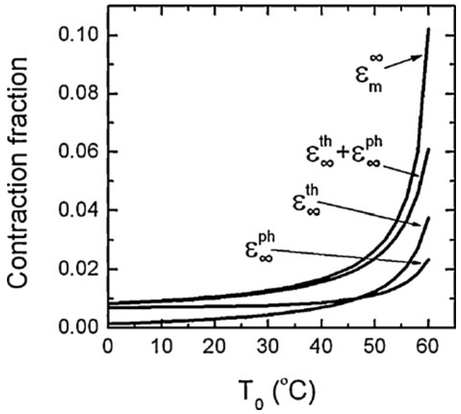

**Fig. 3.** The total contraction $\varepsilon_m^{\infty}$, the photo-induced contraction $\varepsilon_{\infty}^{ph}$, the thermal-induced contraction $\varepsilon_{\infty}^{th}$ and their sum as functions of the environmental temperature $T_0$.

lation $n_c(t)$ and the sample temperature $T(t)$. With $n_c(t)$ determined, the shift of the NI transition temperature can be calculated from (5) and the contractions can be completely evaluated from Eqs. (16) and (17).

For $T_0 = 20\,^{\circ}\mathrm{C} < T_0^c$, the sample temperature increase $\delta T = T - T_0$ is much smaller than the NI transition temperature shift $\delta T_{ni} = T_{ni}^0 - T_{ni}$ as shown in Fig. 4(a). Thus, the thermal-induced contraction $\varepsilon_m^{th}$ is rather small, see Fig. 4(b). However, for $T_0 = 60\,^{\circ}\mathrm{C} > T_0^c$, the situation changes, see Fig. 5. As $\delta T$ gets bigger than $\delta T_{ni}$ due to radiation, the thermal-induced contraction $\varepsilon_m^{th}$ extends the photo-induced contraction $\varepsilon_m^{ph}$. Moreover, Fig. 4(b) shows the total contraction $\varepsilon_m$ approximates the sum of $\varepsilon_m^{th}$ and $\varepsilon_m^{ph}$. The linear approximation is valid at this temperature because of the very small values of the normalized shifts $\delta\theta$ and $\delta\theta_{ni}$.

Still, the nonlinear character of Eq. (18) for $\xi \approx 0.2$ is evident in Fig. 5(b) at higher environment temperatures. To demonstrate this more clearly, Fig. 6 shows the time evolution of (a) the total contraction $\varepsilon_m$, (b) the contraction ratio $\varepsilon_m^{th}/\varepsilon_m^{ph}$ for $T_0 = 20, 40, 50, 55, 60\,^{\circ}\mathrm{C}$. For short time UV light illumination, the thermal-induced contraction $\varepsilon_m^{th}$ is irrelevant. However, after extensive illuminations, it becomes larger than the photo-induced contraction $\varepsilon_m^{ph}$ for $T_0 > T_0^c$. Also, the higher the environmental temperature $T_0$ is, the larger the contraction ratio $\varepsilon_m^{th}/\varepsilon_m^{ph}$.

Both the light-induced contractions and the raising of the temperatures shown in Figs. 4–6 are comparable with the experiments, see Figs. 7 and 8 in [9]. Moreover, the total contractions of Figs. 3 and 6(a) agree quite well with the experimental reported saturated contractions of about 3%, 4% and 7% at $T_0$ = 50, 57 and 59 °C. The shifts of the sample temperatures of Figs. 2 and 6(b) for these oven temperatures are also in good agreement (Figs. 7 and 8 of [9]). However, experiments show a much larger temperature shift and contraction at $T_0$ = 25 °C and this needs to be investigated in the future.

### 3.2. Thermal and photo-induced stresses for clamped samples

When the LCE sample is irradiated by UV light in displacement control mode (clamped sample), the light-induced decrease of the stress-free length results into a stressed sample [10]. For nematic

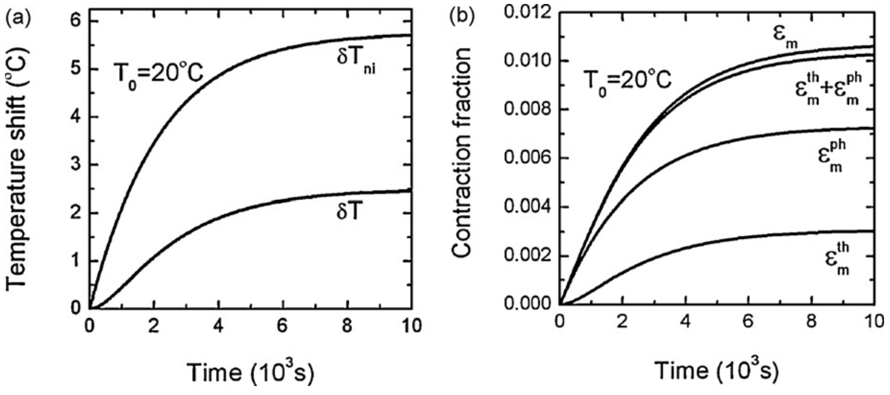

**Fig. 4.** Time evolution of (a) the shifts of sample temperature $\delta T(t) = T(t) - T_0$ and the NI transition temperature $\delta T_{ni}(t) = T_{ni}^0 - T_{ni}(t)$; (b) the total contraction $\varepsilon_m$, the photo-induced contraction $\varepsilon_m^{ph}$, the thermal-induced contraction $\varepsilon_m^{th}$ and their sum.

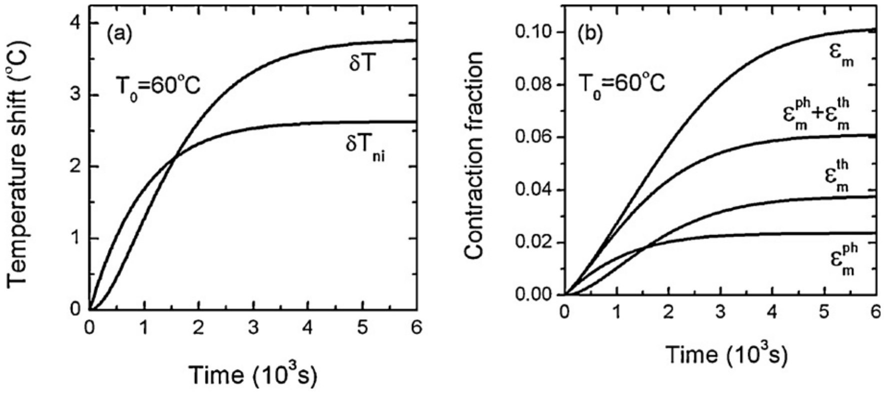

**Fig. 5.** Time evolution of (a) the shifts of sample temperature $\delta T(t) = T(t) - T_0$ and the NI transition temperature $\delta T_{\mathrm{ni}}(t) = T_{\mathrm{ni}}^0 - T_{\mathrm{ni}}(t)$; (b) the total contraction $\varepsilon_{\mathrm{m}}$, the photo-induced contraction $\varepsilon_{\mathrm{m}}^{\mathrm{ph}}$, the thermal-induced contraction $\varepsilon_{\mathrm{m}}^{\mathrm{th}}$ and their sum.

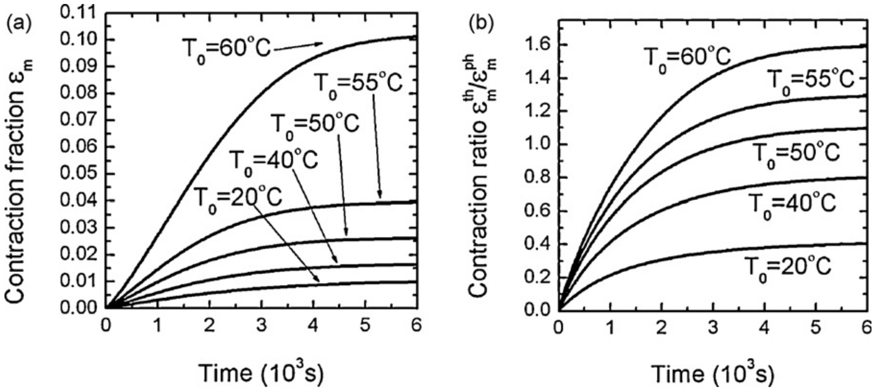

**Fig. 6.** Time evolution of (a) the total contraction $\varepsilon_{\mathrm{m}}$; (b) the ratio $\varepsilon_{\mathrm{m}}^{\mathrm{th}}/\varepsilon_{\mathrm{m}}^{\mathrm{ph}}$ at the environmental temperatures $T_0 = 20, 40, 50, 55, 60\,^\circ$C.

elastomers, the stress-strain relation [1,7,10,25] under uniaxial loading along the director **n** is

$$\sigma = n_{\mathrm{s}}kT\left[\left(\frac{\lambda}{\lambda_{\mathrm{m}}}\right)^2 - \frac{\lambda_{\mathrm{m}}}{\lambda}\right], \tag{21}$$

with $n_{\mathrm{s}}$ the number density of the cross-linked strands, $k$ the Boltzmann constant. For a clamped sample, the uniaxial expansion is fixed as $\lambda \equiv \lambda_0 = 1 + \alpha(T_{\mathrm{ni}}^0 - T_0)^{\xi}$ by (7). Under UV irradiation, the stress-free uniaxial expansion decreases by

$$\lambda_{\mathrm{m}} = 1 + \alpha(T_{\mathrm{ni}} - T)^{\xi} = 1 + \alpha(T_{\mathrm{ni}}^0 - T_0)^{\xi}(1 - \delta\theta - \delta\theta_{\mathrm{ni}})^{\xi}. \tag{22}$$

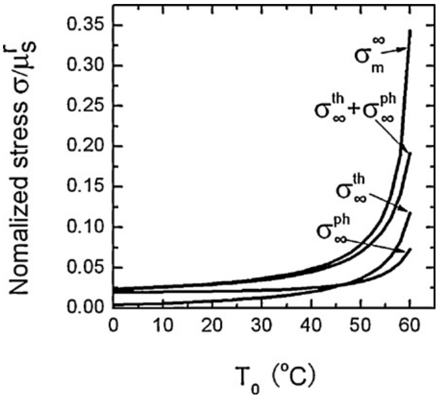

**Fig. 7.** The total stress $\sigma_{\mathrm{m}}^{\infty}$, the photo-induced stress $\sigma_{\infty}^{\mathrm{ph}}$, the thermal-induced stress $\sigma_{\infty}^{\mathrm{th}}$ and their sum as functions of the environmental temperature $T_0$.

As a result, the stress increases. By the elimination of the steady values of the temperature shifts $\delta\theta_\infty$ and $\delta\theta_{\mathrm{ni}}^{\infty}$ from above equation, the steady stress $\sigma_\infty$ after long time irradiation can be calculated by (21). We set $\lambda \equiv \lambda_0$ and plot the result as a function of $T_0$, see Fig. 7. For comparison, the thermal and the photo-induced parts $\sigma_{\infty}^{\mathrm{th}}$ and $\sigma_{\infty}^{\mathrm{ph}}$, as calculated using the uniaxial expansions with $\delta\theta_\infty$ and $\delta\theta_{\mathrm{ni}}^{\infty}$ only are shown as well. The stresses of the clamped sample exhibit similar trends as the stress-free contractions of Fig. 3. In fact, all quantities increase with $T_0$. The thermal effect is small at lower temperature but extends the photo effect at $T_0 > T_0^{\mathrm{c}}$. The evolution processes are calculated as well and they are similar to the results obtained for the unloaded sample (Fig. 6).

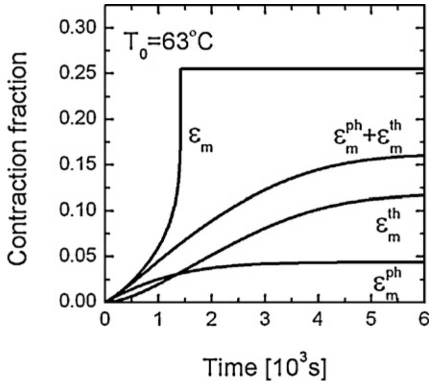

**Fig. 8.** Time evolution of the total contraction $\varepsilon_{\mathrm{m}}$, the photo-induced contraction $\varepsilon_{\mathrm{m}}^{\mathrm{ph}}$, the thermal-induced contraction $\varepsilon_{\mathrm{m}}^{\mathrm{th}}$ and their sum at the environmental temperature $T_0 = 63^\circ C$ close to $T_{\mathrm{ni}}^0 = 67\,^\circ$C.

### 3.3. Behavior close to the initial NI transition point

As shown in Fig. 2, a sample irradiated at $T_0 > T_0^{\mathrm{M}} > T_0^{\mathrm{c}}$ transforms into the isotropic phase after sufficient long UV light exposure since $T_\infty > T_{\mathrm{ni}}$ and the temperature increase $\delta T_\infty = T_\infty - T_0$ is larger than the NI transition temperature shift $\delta T_{\mathrm{ni}}^\infty = T_{\mathrm{ni}}^0 - T_{\mathrm{ni}}^\infty$. Without considering the temperature increase, the sample would remain in the nematic phase until $T_0 = T_1^{\mathrm{M}}$ given by $T_{\mathrm{ni}} = T_0$. Our calculation shows that $T_1^{\mathrm{M}} = 64.6\,^\circ\mathrm{C}$, about $4^\circ$ higher than $T_0^{\mathrm{M}}$.

For $T_0^{\mathrm{M}} < T_0 < T_1^{\mathrm{M}}$, the photo-induced contraction $\varepsilon_{\mathrm{m}}^{\mathrm{ph}}$ is much smaller than the thermal-induced $\varepsilon_{\mathrm{m}}^{\mathrm{th}}$ and the sample enters the isotropic phase after light exposure as shown in Fig. 8 for $T_0 = 63\,^\circ\mathrm{C}$. Similar result is indeed observed in [9]. Both the values of the critical time of light exposure and the saturated contraction are of the same order as of the experiment (Fig. 10 of [9]). Moreover, the total contraction $\varepsilon_{\mathrm{m}}$ is much bigger than their sum due to the strong nonlinearity of the contraction function (16) for very small values of the temperature difference $T_{\mathrm{ni}} - T$. It is obvious that the effect of the sample temperature increase must be taken into account due to its strong contribution to the total contraction.

## 4. Conclusions

A model is proposed for the calculation of the temperature changes during the recently reported photo-mechanical processes in liquid crystal elastomers. In addition to the power of the external force and the heat conduction, the rate of the temperature can be strongly affected by the light illumination through direct heating and self-heating. The self-heating considered here is resulted from the thermally activated back conversion of the azo dyes from the metastable *cis* state to the stable *trans* state. Numerical calculations indicated that there is a critical temperature $T_0^c$, below which the NI transition temperature shift induced by the photo-isomerization plays the main role for the observed stress-free sample contractions and the stress increase of clamped samples. However, when the environmental temperature is higher than $T_0^{\mathrm{c}}$, the temperature increase is more pronounced and thus affects a larger contribution to the contractions and/or stresses than the NI transition temperature shift. This thermal effect is particularly important for temperatures close to the initial NI transition temperature. Therefore, our theoretical results motivate a need for more accurate calorimetrical measurements to the study of the newly reported photo-mechanical effects of LCEs in greater detail.

## Acknowledgment

We are grateful to the support of National Science Foundation of China (10672042, 10772049).

## References

[1] M. Warner, E.M. Terentjev, Liquid Crystal Elastomers, Clarendon Press, Oxford, 2003.
[2] P.G. de Gennes, M. Hebert, R. Kant, Macromol. Symp. 113 (1997) 39–49.
[3] A.R. Tajbakhsh, E.M. Terentjev, Eur. Phys. J. E 6 (2001) 181–188.
[4] S.M. Clarke, A. Hotta, R.R. Tajbakhsh, E.M. Terentjev, Phys. Rev. E 64 (2001) 061702.
[5] M.H. Li, P. Keller, Philos. Trans. R. Soc. A 364 (2006) 2763–2777.
[6] H. Finkelmann, S.T. Kim, A. Munoz, P. Palffy-Muhoray, B. Taheri, Adv. Mater. 13 (2001) 1069–1072.
[7] P. Bladon, M. Warner, E.M. Terentjev, Macromolecules 27 (1994) 7067–7075.
[8] H. Finkelmann, E. Nishikawa, G.G. Pereira, M. Warner, Phys. Rev. Lett. 87 (2001) 1–4, 015501.
[9] P.M. Hogan, A.R. Tajbakhsh, E.M. Terentjev, Phys. Rev. E 65 (2002) 1–10, 041720.
[10] J. Cviklinski, A.R. Tajbakhsh, E.M. Terentjev, Eur. Phys. J. E 9 (2002) 427–434.
[11] Y. Yu, M. Nakano, T. Ikeda, Nature 425 (2003) 145–1145.
[12] M. Camacho-Lopez, H. Finkelmann, P. Palffy-Muhoray, M. Shelley, Nat. Mater. 3 (2004) 307–310.
[13] T.J. White, N.V. Tabiryan, S.V. Serak, U.A. Hrozhyk, V.P. Tondiglia, H. Koerner, R.A. Vaia, T.J. Bunning, Soft Matt 4 (2008) 1796–1798.
[14] T. Ikeda, J. Mater. Chem. 13 (2003) 2037–2057.
[15] V. Shibaey, A. Bobrovsky, N. Borko, Prog. Polym. Sci. 28 (2003) 729–836.
[16] M. Warner, L. Mahadevan, Phys. Rev. Lett. 92 (2004), 134302 1-4.
[17] L. Jin, X. Jiang, Y. Huo, Sci. China 49 (2006) 553–563.
[18] Z.Y. Wei, L.H. He, J. Chem. Phys. 124 (2006), 064708 1-7.
[19] I. Janossy, L. Szabados, Phys. Rev. E 58 (1998) 4598–4604.
[20] C.L.M. Harvey, E.M. Terentjev, Eur. Phys. J. E 25 (2007) 185–189.
[21] T. Hugel, N.B. Holland, A. Cattani, L. Moroder, M. Seitz, H. Gaub, Science 296 (2002) 1103–1106.
[22] C.D. Eisenbach, Polymer 21 (1980) 1175–1179.
[23] S. Monti, G. Orlandi, P. Palmieri, Chem. Phys. 71 (1982) 87–99.
[24] H. Rau, J. Photochem. 26 (1984) 221–225.
[25] H. Finkelmann, A. Greve, M. Warner, Eur. J. Phys. E 5 (2001) 281–293.
[26] G. Feio, J.L. Figueirinhas, A.R. Tajbakhsh, E.M. Terentjev, 78 (2008) 020201.
[27] K.K. Hon, D. Corbett, E.M. Terentjev, Eur. Phys. J. E 25 (2008) 83–89.